Generalised meshes for quantum mechanical problems

1986 J. Phys. A: Math. Gen. 19 2041

(http://iopscience.iop.org/0305-4470/19/11/013)

J. Phys. A: Math. Gen. **19** (1986) 2041-2059. Printed in Great Britain

Generalised meshes for quantum mechanical problems

D Baye and P-H Heenen†

Physique Théorique et Mathématique CP 229, Université Libre de Bruxelles, 1050 Brussels, Belgium

Received 18 July 1985, in final form 14 November 1985

Abstract. A new method to discretise Schrödinger equations on a mesh is described. This method is based on an accurate approximation of a variational calculation. The regularly spaced mesh and meshes based on the zeros of orthogonal polynomials are studied in detail. It is shown that with each type of mesh is associated a particular kinetic energy operator and an optimal formula for its discretised form. The applications to some simple potential problems show that the method is very accurate as well as very simple. Applications to many-body problems indicate that the accuracy of the results is improved by an order of magnitude with respect to conventional mesh calculations.

1. Introduction

Many-body problems in atomic and nuclear physics have been studied for more than ten years by means of methods which use a coordinate mesh. Most of the studies have been performed within the mean-field approximation. The time-dependent Hartree-Fock method has been applied to atomic collisions with a cylindrical symmetry (Sandhya Devi and Garcia 1983) and to nuclear collisions in three dimensions (Flocard *et al* 1978, for a review see Negele 1982). Very recently, new discretisation schemes have been developed (Bonche *et al* 1985) and have permitted the study of the static deformation properties of triaxial nuclei with a much better calculational accuracy than that which is achieved by expanding the individual wavefunctions in terms of an oscillator basis. Other applications, going beyond the mean-field approximation, such as the study of the mixing of different configurations by means of the generator coordinate method (Marcos *et al* 1983) and calculations to achieve the restoration of rotational invariance (Baye and Heenen 1984), have also been successfully carried out for problems in nuclear physics. However, despite the success of calculations which employ meshes, discretised equations have not been derived in a completely convincing manner and many questions which were raised in the first applications of such methods (Hoodbhoy and Negele 1977) have still not been answered. The aim of this paper is to set calculations using a mesh on firmer ground. To this end, we will be led to modify and generalise the discretisation procedures. We will then show that they provide a very simple and very accurate method of solution of the Schrödinger equation.

† Maître de Recherches FNRS.

0305-4470/86/112041+19$02.50

Let us first recall how finite difference equations on a mesh are derived (Negele 1982). The full many-body Schrödinger equation follows from varying the action

$$S = \int \mathrm{d}t \int \mathrm{d}\vec{r}_1 \ldots \mathrm{d}\vec{r}_n [\Psi^*(\vec{r}_1 \ldots \vec{r}_n, t)(\mathrm{i}\,\partial/\partial t - H)\Psi(\vec{r}_1 \ldots \vec{r}_n, t)]. \quad (1.1)$$

In the mean-field approximation, the many-body wavefunction Ψ is parametrised as a Slater determinant. The action is then rewritten and becomes a functional depending on the individual wavefunctions and their derivatives.

A calculation on a mesh is performed by evaluating approximate values of the wavefunction at fixed points. Up to now, only cartesian meshes, i.e. with a constant spacing between the mesh points, in either cartesian or cylindrical coordinates have been considered. The terms in the action S are then treated in various ways. The time evolution is accomplished by a unitary approximation to the evolution operator. In this paper, we shall not study this evolution, although the method that we present can also be applied to the time derivative. The integrals over the individual coordinates are approximated by a rectangle formula (the same weight is taken for all the points). The second-order derivatives in the kinetic energy term (and possibly the first-order derivatives in the spin-orbit contribution) are approximated by finite-difference formulae using various numbers of points. In this way, the action is expressed as a function of the values of the wavefunction at the mesh points. The variational equations on the mesh follow from varying S with respect to these values. This procedure leads to a matrix equation, which is solved by iterative methods.

In Hartree-Fock calculations, the three-dimensional (3D) cartesian mesh leads to very accurate results when large-order finite-difference formulae approximate the derivatives (Bonche *et al* 1985). However, this approach presents several shortcomings and unexplained properties.

(i) Calculations on a mesh are not expected to provide upper bounds of the exact energy of the problem. The variational behaviour of the Hartree-Fock method seems thus to be lost when the equations are discretised on a mesh.

(ii) Tests have shown that the rectangle integration formula unexpectedly leads to more accurate results than those obtained from more sophisticated integration procedures.

(iii) Although very large mesh sizes provide accurate results on 3D cartesian meshes (e.g. 1 fm in nuclear physics applications), the use of a much smaller mesh size seems to be necessary for the polar coordinate of cylindrical meshes (Hoodbhoy and Negele 1978, Sandhya Devi and Garcia 1983).

(iv) Non-equally spaced mesh points could be a more judicious choice for some physical applications. The procedure explained above has no evident generalisation.

(v) The wavefunctions are only known at the mesh points, with the consequence that a change in the mesh size requires a full new calculation.

In an attempt to answer these questions, we present in this paper a new derivation of equations on a mesh. The principle of the method is to apply the variational principle to a trial function in which the mesh points play a special role. After the introduction of an accurate approximation, mesh equations are derived without loss of the usual simplicity of mesh calculations. In § 2, we present the method for 1D potential problems. The generalisation to several dimensions is very simple and the principle of the method remains valid for mean-field calculations. In § 3, we study the properties of different families of meshes. In particular, we show that our derivation gives an answer to the questions that we have raised for the cartesian mesh. We also investigate in § 4 the

accuracy obtained for different simple quantum mechanical problems. In § 5, we apply our method to the calculation of nuclear Hartree-Fock energies and to the rotation on a mesh of Slater determinants.

2. The Lagrange meshes and their variational foundation

As explained in the introduction, we focus on a one-dimensional Schrödinger equation with a local potential $V(x)$

$$(T+V(x))\Psi(x)=E\Psi(x) \qquad x\in(a,b). \tag{2.1}$$

The variable x may represent, e.g., a cartesian, polar, radial or angular coordinate. One or both limits of the interval (a, b) can thus be infinite. The self-adjoint kinetic energy operator T is defined in accord with the choice of x. It may contain terms other than derivatives. Examples of choices of x and T are given in the next paragraph.

In a calculation on a mesh, one only considers the values $\Psi(x_j)$ of the wavefunction $\Psi(x)$ at N given points x_j. Here, we shall make use of continuous functions but the $\Psi(x_j)$ will play a special role. Let us introduce a set of N Lagrange functions $f_i(x)$ satisfying the two conditions

$$f_i(x_j)=\delta_{ij} \tag{2.2}$$

and

$$\int_a^b f_i^*(x)f_j(x)\,\mathrm{d}x=\lambda_i\delta_{ij}. \tag{2.3}$$

The first condition is the usual one encountered in Lagrange interpolation. It provides an approximation of the wavefunction based on its value at the mesh points, namely

$$\Psi(x)=\sum_{i=1}^{N}\Psi(x_i)f_i(x). \tag{2.4}$$

The orthogonality condition (2.3) is essential in order to associate a simple and accurate scalar product formula with the mesh. The scalar product of two functions of the form (2.4) is given exactly by

$$\int_a^b \Phi^*(x)\Psi(x)\,\mathrm{d}x=\sum_{i=1}^{N}\lambda_i\Phi^*(x_i)\Psi(x_i). \tag{2.5}$$

Notice that (2.3) is not satisfied by the usual Lagrange interpolation polynomials and thus requires the introduction of more specialised interpolation functions.

The expression (2.5) for the scalar product is a particular case of the generalised Gauss quadrature formula

$$\int_a^b F(x)\,\mathrm{d}x\approx\sum_{i=1}^{N}\lambda_iF(x_i). \tag{2.6}$$

With (2.3), one verifies that (2.6) is exact for any product $f_i^*f_j$. We shall see in § 3.2 that this formula contains the usual Gauss quadrature for particular choices of the mesh. Equation (2.6) also shows that the λ_i can be interpreted as generalised Christoffel numbers (Szegö 1967) associated with the mesh.

In order to determine Lagrange functions, we consider a set of N basis functions $\varphi_k(x)$ orthonormal on (a, b)

$$\int_a^b \varphi_k^*(x)\varphi_l(x)\,\mathrm{d}x = \delta_{kl} \qquad k, l = 0 \text{ to } N-1. \tag{2.7}$$

It is readily seen that functions f_i satisfying the conditions (2.2) and (2.3) can be constructed by combining linearly the functions φ_k if and only if the matrix with $\lambda_i^{1/2}\varphi_k(x_i)$ as a general element is unitary. The existence condition of a Lagrange mesh is thus

$$\sum_{k=0}^{N-1} \varphi_k^*(x_i)\varphi_k(x_j) = \lambda_i^{-1}\delta_{ij}. \tag{2.8}$$

For a given set of functions φ_k, the N mesh points x_i must verify $\frac{1}{2}N(N-1)$ conditions. The N remaining conditions (2.8) determine the Christoffel numbers

$$\lambda_i = \left(\sum_{k=0}^{N-1} |\varphi_k(x_i)|^2\right)^{-1}. \tag{2.9}$$

If conditions (2.8) are satisfied, the Lagrange functions are given by

$$f_i(x) = \lambda_i \sum_{k=0}^{N-1} \varphi_k^*(x_i)\varphi_k(x). \tag{2.10}$$

Relation (2.10) can be inverted as

$$\varphi_k(x) = \sum_{i=1}^{N} \varphi_k(x_i) f_i(x). \tag{2.11}$$

The Gauss formula (2.6) is thus exact for any product of the form $\varphi_k^*\varphi_l$.

In order to derive an approximate Schrödinger equation on the mesh, we use the form (2.4) as a trial function in a variational calculation. The values $\Psi(x_j)$ are thus nothing but linear variational coefficients. Here it is more convenient to work with the normalised functions $\lambda_i^{-1/2} f_i(x)$. The matrix elements of the kinetic energy operator are calculated exactly:

$$T_{ij} = (\lambda_i\lambda_j)^{-1/2} \int_a^b f_i^*(x)\, T f_j(x)\,\mathrm{d}x. \tag{2.12}$$

Notice that this matrix element has to be determined only once for each family of Lagrange functions. Examples are given in the next paragraph. The matrix elements of the potential are approximated with the Gauss quadrature (2.6) as

$$(\lambda_i\lambda_j)^{-1/2} \int_a^b f_i^*(x)\, V(x) f_j(x) \approx V(x_i)\delta_{ij} \tag{2.13}$$

because of (2.2). Notice that (2.13) is not always an approximation (see §§ 4.3 and 4.4).

The Schrödinger equation (2.1) reduces to the matrix equation

$$\sum_j (T_{ij} + V(x_i)\delta_{ij})\lambda_j^{1/2}\Psi(x_j) = E\lambda_i^{1/2}\Psi(x_i) \tag{2.14}$$

where only values of the wavefunction at the mesh points appear. Equation (2.14) has the usual form—and especially the usual simplicity—of an equation discretised on a mesh. It has however several advantages. It is based on a variational principle

(although approximation (2.13) introduces a slight breaking of the variational procedure) and the wavefunction is defined by (2.4) at any point of the interval (a, b). A more convenient form of (2.14) is obtained by introducing a scale factor h—the mesh size—in the equation

$$\sum_j (h^{-2}T_{ij} + V(hx_i)\delta_{ij})\lambda_j^{1/2}\Psi(hx_j) = E\lambda_i^{1/2}\Psi(hx_i) \tag{2.15}$$

where T_{ij} and x_i are now dimensionless. This form of the kinetic energy matrix element T_{ij} can be tabulated for each type of mesh. All formulae in the following are presented with $h = 1$.

3. Types of Lagrange meshes

3.1. Cartesian mesh

The cartesian mesh is the most natural mesh. Here, we show that it is linked with Fourier basis functions and this fact enables us to derive formulae for the kinetic energy which improve the accuracy of usual cartesian mesh calculations.

The N Fourier basis functions

$$\varphi_k(x) = N^{-1/2}\exp[\mathrm{i}(2\pi k/N)x] \tag{3.1}$$

(where k varies from $-\frac{1}{2}(N-1)$ to $\frac{1}{2}(N-1)$ by unit steps) are orthonormal over the interval $(-\frac{1}{2}N, \frac{1}{2}N)$. The identity

$$\sum_k \varphi_k^*(x)\varphi_k(y) = \frac{1}{N}\frac{\sin \pi(x-y)}{\sin[\pi(x-y)/N]} \tag{3.2}$$

shows that conditions (2.8) are satisfied if the quantities $|x_i - x_j|$ are integers smaller than N. The Fourier functions are thus associated with a cartesian mesh whose abscissae vary as k from $-\frac{1}{2}(N-1)$ to $\frac{1}{2}(N-1)$ (see figure 1 in Baye and Heenen (1984)). Moreover, (2.9) and (3.2) provide the Christoffel numbers

$$\lambda_i = 1. \tag{3.3}$$

In this case, the Gauss quadrature formula (2.6) is nothing but the rectangle rule. As discussed in § 2, this formula is exact for $\varphi_k^*\varphi_l$, i.e. for functions of the form $\cos(2\pi nx/N)$ where n is an integer comprised between 0 and $N-1$ (see Bakhvalov 1973). Besides, it is exact for any odd function. The unexpected accuracy of the rectangle formula, discussed in the introduction, receives a simple explanation here.

With (3.2), the expression (2.10) can be summed and provides the diffraction-like Lagrange functions

$$f_i(x) = \frac{1}{N}\frac{\sin \pi(x-i)}{\sin[\pi(x-i)/N]}. \tag{3.4}$$

These functions are well adapted to the kinetic energy $T = -\mathrm{d}^2/\mathrm{d}x^2$. One has

$$\begin{aligned} T_{ij} &= -f_i''(j) = -f_j''(i) \\ &= \begin{cases} \dfrac{\pi^2}{3}\left(1 - \dfrac{1}{N^2}\right) & i = j \\ (-1)^{i-j}\dfrac{2\pi^2}{N^2}\dfrac{\cos[\pi(i-j)/N]}{\sin^2[\pi(i-j)/N]} & i \neq j. \end{cases} \end{aligned} \tag{3.5}$$

The first equality arises from the fact that $f_i''(x)$ is a linear combination of functions $\varphi_k(x)$. The Gauss formula (2.6) is then exact for this matrix element. The other equalities are obtained with elementary calculations. The formulae (3.5) represent expressions for the kinetic energy which are coherent with the cartesian mesh. The formulae which are usually employed in calculations on a cartesian mesh can be considered as more or less accurate approximations of (3.5).

The formulae that we have discussed here can also be encountered in different contexts. They are related to the discrete Fourier transform (Bakhvalov 1973). The basis functions φ_k also correspond to the simplest type of polynomials orthogonal on the unit circle (Szegö 1967). The cartesian mesh is therefore the optimal mesh to discretise the azimuthal angle φ. Further meshes (corresponding to more complicated kinetic energy operators) can be derived from other types of such polynomials. However, more useful meshes are associated with orthogonal polynomials on a real interval as we now show.

3.2. Meshes related to orthogonal polynomials

3.2.1. General formulae. Let us consider a family of orthogonal polynomials $p_k(x)$ associated with a weight function $w(x)$ defined on (a, b). Functions $\varphi_k(x)$ can then be defined as

$$\varphi_k(x) = h_k^{-1/2} p_k(x) w(x)^{1/2} \tag{3.6}$$

where $h_k^{1/2}$ is the norm of p_k. With the Christoffel-Darboux formula (Szegö 1967), these functions satisfy the relation

$$\sum_{k=0}^{N-1} \varphi_k(x)\varphi_k(y) = \frac{k_{N-1}}{k_N}\left(\frac{h_N}{h_{N-1}}\right)^{1/2} \frac{\varphi_N(x)\varphi_{N-1}(y) - \varphi_{N-1}(x)\varphi_N(y)}{x-y} \tag{3.7}$$

where k_n is the coefficient of x^n in $p_n(x)$. With (3.7), it is readily seen that the condition (2.8) of existence of a mesh is fulfilled for abscissae x_i satisfying

$$p_N(x_i) = 0. \tag{3.8}$$

A mesh can thus be associated with every family of orthogonal polynomials. With (2.2), (2.10), (3.7) and (3.8), the corresponding Lagrange functions are then easily shown to be

$$f_i(x) = \frac{1}{\varphi_N'(x_i)} \frac{\varphi_N(x)}{x - x_i}. \tag{3.9}$$

Every function is the product of a polynomial of degree $N-1$ by $w^{1/2}$. With (2.9) and (3.7), the coefficients λ_i are obtained as

$$\lambda_i = \frac{k_N}{k_{N-1}}\left(\frac{h_{N-1}}{h_N}\right)^{1/2} (\varphi_N'(x_i)\varphi_{N-1}(x_i))^{-1}. \tag{3.10}$$

These coefficients differ from those of equation (3.4.7) in Szegö (1967) by the fact that they include the weight factor $w(x)$. The Gauss quadrature formula (2.6) can then be written in the present notation as

$$\int_a^b P(x)w(x)\,\mathrm{d}x \approx \sum_i \lambda_i P(x_i) w(x_i). \tag{3.11}$$

Equation (3.11) is exact if $P(x)$ is a polynomial whose degree is not larger than $2N-1$ (Szegö 1967). The domain of validity is thus more extended than the one obtained in § 2.

Now we particularise the present formulae to a few meshes which have an obvious physical importance.

3.2.2. Hermite mesh. This mesh is expected to be useful for one-dimensional Schrödinger equations with

$$T = -\mathrm{d}^2/\mathrm{d}x^2 \tag{3.12}$$

since the definition interval of the Hermite polynomials $H_n(x)$ is $(-\infty, +\infty)$. The weight function is $w(x) = \exp(-x^2)$.

The properties of the Hermite polynomials and the expressions of the constants h_n and k_n are given in Abramowitz and Stegun (1965). They lead to

$$\lambda_i = 2/\varphi'_N(x_i)^2 \tag{3.13}$$

where x_i is a zero of $H_N(x)$. The matrix elements of T involve the second derivative of $\lambda_i^{-1/2} f_i(x) = (-1)^i 2^{-1/2}(x - x_i)^{-1}\varphi_N(x)$. Because of the derivatives of $w^{1/2}$ in φ_N, the integrand in the expression of T_{ij} is the product of w by a polynomial of degree $2N$. After subtraction of the expression $(-1)^{i-j}\frac{1}{2}H_N(x)^2 \exp(-x^2)$ (whose integral is immediate), the remaining term is proportional to a polynomial of degree $2N-1$ for which the Gauss formula (3.11) is exact. The calculation of T_{ij} then becomes straightforward and gives the simple result

$$T_{ij} = \begin{cases} \frac{1}{6}(4N - 1 - 2x_i^2) & i = j \\ (-1)^{i-j}[2(x_i - x_j)^{-2} - \frac{1}{2}] & i \neq j. \end{cases} \tag{3.14}$$

3.2.3. Laguerre mesh. Since the definition interval of the Laguerre polynomials is $(0, \infty)$, we expect the corresponding mesh to be useful for polar or radial coordinates. We shall consider the generalised Laguerre polynomials $L_n^\alpha(x)$ associated with the weight function $x^\alpha \mathrm{e}^{-x}$ and with the kinetic energy operator

$$T = -\frac{\mathrm{d}^2}{\mathrm{d}x^2} + \frac{\alpha(\alpha - 2)}{4x^2}. \tag{3.15}$$

Obviously, the values $\alpha = 2l + 2$ correspond to the kinetic energy of the radial motion in spherical coordinates for a given orbital momentum l. The important property is that the highly singular centrifugal term is included in T so that its matrix elements will be exactly calculated. The odd integer values $\alpha = 2|m| + 1$ correspond to the kinetic energy in polar coordinates for a given magnetic quantum number m. Again, the centrifugal term is included. The Lagrange functions present the striking property of behaving like $x^{\alpha/2}$ for small x values. The correct behaviour r^{l+1} in spherical coordinates or $r^{|m|+1/2}$ in polar coordinates is exactly reproduced. Notice however that the mesh will be different for every l or m value.

With the formulae of Abramowitz and Stegun (1965), one obtains

$$\lambda_i = 1/(x_i \varphi'_N(x_i)^2) \tag{3.16}$$

where x_i is a zero of $L_N^\alpha(x)$. The matrix elements of T are again calculated with the exact formula (3.11). Some complications arise because of the derivatives of $w^{1/2}$ which are not products of $w^{1/2}$ by polynomials. This difficulty can be eliminated by integrating by parts. However, the matrix elements are less simple than in the other cases

$$T_{ij} = \begin{cases} (\alpha + 1)^2/4x_i^2 + S_{ii} & i = j \\ (-1)^{i-j}[\frac{1}{2}(\alpha + 1)(x_i x_j)^{-1/2}(x_i^{-1} + x_j^{-1}) + S_{ij}] & i \neq j \end{cases} \tag{3.17}$$

with

$$S_{ij} = (x_i x_j)^{1/2} \sum_{k \neq i,j} x_k^{-1} (x_k - x_i)^{-1} (x_k - x_j)^{-1}.$$

3.2.4. Legendre mesh. The Legendre mesh is especially useful for the case $x = \cos\theta$. The kinetic energy operator corresponding to the angular momentum operator $\boldsymbol{L}^2$ is

$$T = -\frac{\mathrm{d}}{\mathrm{d}x}(1-x^2)\frac{\mathrm{d}}{\mathrm{d}x} + \frac{m^2}{1-x^2} \tag{3.18}$$

for a given value of the magnetic quantum number m. The basis functions φ_k are constructed by normalising the associated Legendre functions $P_{|m|+k}^{|m|}(x)$. Since these functions are related to Jacobi polynomials, one easily shows that they satisfy the Christoffel-Darboux formula (3.7).

The Christoffel numbers are given by

$$\lambda_i = (2N + 2|m| + 3)/[(1-x_i^2)\varphi'_N(x_i)^2] \tag{3.19}$$

where the x_i are the zeros of $P_{|m|+k}^{|m|}$. The matrix elements of T are straightforwardly shown to be

$$T_{ij} = \begin{cases} \frac{1}{3}(N+|m|+1)(N+|m|+2) + \frac{2}{3}(m^2-1)(1-x_i^2)^{-1} & i = j \\ (-1)^{i-j} 2(1-x_i^2)^{1/2}(1-x_j^2)^{1/2}(x_i - x_j)^{-2} & i \neq j. \end{cases} \tag{3.20}$$

The mesh points depend of course on the selected $|m|$ values. The eigenvalues of the matrix (T_{ij}) are exactly those of $\boldsymbol{L}^2$, i.e. they take the form $(|m|+n)(|m|+n+1)$ where n is an integer smaller than N.

3.3. Modified meshes

3.3.1. Principle. Let us start with the mesh points x_i associated with basis functions $\tilde{\varphi}_k(x)$ defined on (a, b) which verify the existence condition (2.8). Let ρ be a monotonously increasing function belonging to $C^3(a, b)$. Then the functions

$$\varphi_k(x) = (\mathrm{d}\rho/\mathrm{d}x)^{1/2} \tilde{\varphi}_k(\rho(x)) \tag{3.21}$$

also satisfy (2.7) and (2.8). They correspond to a new mesh defined by

$$x_i = \rho^{-1}(\tilde{x}_i). \tag{3.22}$$

Apparently, with (3.22), it is possible to associate a set of functions φ_k with any mesh. However, the differential equations corresponding to the functions φ_k do not in general lead to a physically interesting kinetic energy operator. The present extension of the mesh types may nevertheless be useful in some cases as shown in the next subsection.

3.3.2. Modified Laguerre mesh. We apply (3.21) to Laguerre basis functions with $\rho(x) = x^2$. The basis functions are then

$$\varphi_k(x) = (h_k)^{-1/2} x^{\alpha+1/2} L_k^{\alpha}(x^2) \exp(-\tfrac{1}{2}x^2). \tag{3.23}$$

It is readily seen that these functions correspond to a kinetic energy operator

$$T = -\frac{\mathrm{d}^2}{\mathrm{d}x^2} + \frac{\alpha^2 - \frac{1}{4}}{x^2}. \tag{3.24}$$

Notice that the physical α values differ from those of § 3.2.3. The values $\alpha = l + \frac{1}{2}$ correspond to a radial equation with orbital momentum l and $\alpha = |m|$ to polar equations with azimuthal quantum number m. Here also, the Lagrange functions present the correct behaviour r^{l+1} or $r^{|m|+1/2}$ near $r = 0$.

The Lagrange functions are defined as

$$f_i(x) = \frac{2x_i}{\varphi'_N(x_i)} \frac{\varphi_N(x)}{x^2 - x_i^2} \tag{3.25}$$

where x_i is the positive square root of the zeros of $L_N^{\alpha}(x)$. The Christoffel numbers are given by

$$\lambda_i = 4/\varphi'_N(x_i)^2. \tag{3.26}$$

The matrix elements of T are obtained as

$$T_{ij} = \begin{cases} \frac{2}{3}[\alpha + 2N + 1 + (\alpha^2 - 1)x_i^{-2} - \frac{1}{2}x_i^2] & i = j \\ (-1)^{i-j} 8 x_i x_j / (x_i^2 - x_j^2) & i \neq j. \end{cases} \tag{3.27}$$

4. Application to simple quantum mechanical problems

4.1. One-dimensional harmonic oscillator

The potential $V(x) = x^2$ can be studied either on the cartesian mesh or on the Hermite mesh. Let us first consider the latter mesh which should be particularly well adapted to the harmonic oscillator problem and which illustrates very well the close relationship between calculations on a mesh and on a basis. The calculation with N mesh points provides a striking result when the scale factor h is chosen equal to one: $N-1$ eigenvalues are equal to $2n+1$ ($n = 0$ to $N-2$) and are thus exact whereas the Nth eigenvalue is $\frac{3}{2}N - 1$. The quasi-exactness of the Hermite mesh results can be understood as follows. The Lagrange functions and the functions φ_k are equivalent bases related by an orthogonal transformation. The functions φ_k are the exact eigenfunctions of the problem for $h = 1$. The only approximation in the calculation is the use of the Gauss formula (3.11) to calculate the matrix elements of x^2. Since this formula is exact in this case for all the $\varphi_k \varphi_l$ except φ_{N-1}^2, all the eigenvalues but one must be exact. In spite of its extreme simplicity, the mesh calculation is thus almost equivalent to a variational calculation performed with the functions φ_k. It is instructive to calculate the matrix element of x^2 in the Lagrange basis:

$$(\lambda_i \lambda_j)^{-1/2} \int_{-\infty}^{+\infty} f_i x^2 f_j \, \mathrm{d}x = x_i^2 \delta_{ij} + \tfrac{1}{2}(-1)^{i-j}. \tag{4.1}$$

The term $x_i^2 \delta_{ij}$ corresponds to the approximation of the potential on the mesh (see (2.13)). The second term is due to the fact that the Gauss formula is not valid for φ_{N-1}^2. The neglect of the second term makes the trace of the matrix incorrect and explains the value of the Nth eigenvalue. Notice that the Gauss formula is not a very good approximation for each of the matrix elements given by (4.1). The absolute error is $\frac{1}{2}$. However, the error on the eigenvalues of the matrix on the mesh is zero for most of them. Some eigenvalues, obtained in mesh calculations, can thus be much more accurate than the approximation (2.13) on the potential matrix elements.

We now turn to the cartesian mesh. Figure 1 depicts as full lines the absolute accuracy on the eigenvalues obtained with the cartesian mesh and formula (3.5) for T_{ij}. For $N = 10$, the absolute errors on the first three eigenvalues are smaller than 10^{-3}. For $N = 50$, the first fifteen eigenvalues are obtained to the accuracy of the computer. Beyond $n = 14$, the accuracy becomes progressively worse but remains better than 10^{-3} for $n = 30$. More than half the eigenvalues of the matrix are thus significant! The excellent quality of these results is better illustrated by a comparison with traditional mesh calculations. The broken and dotted lines in figure 1 represent respectively the eigenvalues obtained with traditional 3- and 9-point finite-difference formulae. With the 3-point formula (see equation (25.3.23) in Abramowitz and Stegun 1965), only one ($N = 10$) or two ($N = 50$) eigenvalues have an accuracy better than 10^{-2}. With the 9-point formula, these numbers become four and twelve respectively. The accuracy of the lowest eigenvalue with the 9-point formula is no better than the accuracy of the 24th eigenvalue calculated with (3.5).

The different calculations presented in figure 1 are performed with the optimal choice for the scale parameter h. The present example provides an indication of the way one can choose h when the exact results are not known. The lowest eigenvalues, obtained to the accuracy of the computer, are not very sensitive to the value of h. In contrast, high eigenvalues (say $n = 30$ for example) are very sensitive to it. Since the mesh calculation is an approximate variational calculation, the variation of the 30th eigenvalue with h presents a marked minimum around $h = 0.35$. The optimal choice for h can be obtained by minimising as many of the lowest eigenvalues as possible.

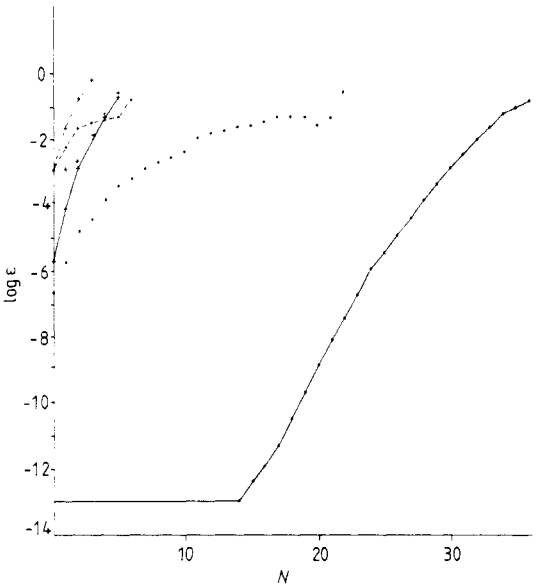

Figure 1. Absolute error on the eigenvalues of the oscillator potential obtained with a cartesian mesh. The crosses correspond to a 10 mesh point calculation, the black points to a 50 mesh point calculation. The full, broken and dotted lines correspond respectively to formula (3.5), a 3-point and a 9-point formula for the kinetic energy.

4.2. Anharmonic potential x^2+x^4

The usefulness of the cartesian and Hermite meshes is now studied in a problem for which an exact analytical solution is not known, i.e. for the potential $V(x)=x^2+x^4$. In table 1 results are presented for 10 and 50 mesh points. For the cartesian mesh, the optimal values for the mesh size are $h=0.55$ ($N=10$) and $h=0.20$ ($N=50$). For the Hermite mesh they are $h=0.60$ in both cases. The absolute accuracy on the zeros of the Hermite polynomial $H_N(x)$ is about 10^{-13} up to $N=50$. The average accuracy is estimated by checking the sum rule

$$\sum_{i=1}^{N} x_i^2=\tfrac{1}{2}N(N-1). \tag{4.2}$$

For $N=10$, the accuracy on the lowest eigenvalue is about 10^{-6} for the Hermite mesh and better than 10^{-5} for the cartesian mesh. The sixth eigenvalue is still obtained to 0.5%. For $N=50$, the four eigenvalues for which accurate values exist (Fernandez *et al* 1985) are obtained with an accuracy better than 10^{-12} with the cartesian mesh. The Hermite mesh gives slightly less accurate results because of the error on the Hermite zeros. The same quality of results is provided for both meshes up to $n=10$. Higher eigenvalues become progressively less accurate but the $n=30$ eigenvalue is still significant.

Table 1. Eigenvalues for $V(x)=x^2+x^4$.

n	$N=10$	$N=50$
0	1.392 342/50	1.392 351 641 531/5/0[a]
1	4.648 80/74	4.648 812 704 213/2/2
2	8.657/6	8.655 049 957 760/59/59
3	13.160/50	13.156 803 898 051/47/50
4	17.961/18.063	18.057 557 436 302/1
5	23.19/31	23.297 441 451 223/3
10		53.449 102 139 666/8
15		88.610 348 800 789/813
20		127.617 777 531/8031/7795[b]
25		169.817 81/78/53
30		214.49/74/78

Results with cartesian mesh/Hermite mesh/exact.

[a] Exact results from Fernandez *et al* (1985).

[b] Exact results from calculations with $N=70$ and 80.

4.3. Two- and three-dimensional harmonic oscillators

The two- and three-dimensional harmonic oscillators can be treated in a unified way. They only differ by the value of the parameter α defined in §§ 3.2.3 and 3.3.2. The modified Laguerre mesh of § 3.3.2 is 'perfect' for this problem. Indeed, it is readily seen that the formula (2.13) is exact for the matrix element of r^2. The mesh calculation is then exact for $h=1$ since the functions φ_k are then the eigenfunctions of the Hamiltonian.

The same problem can also be treated with the Laguerre mesh of § 3.2.3. The accuracy on the Laguerre zeros is better than 10^{-12} for $N=50$ as estimated from the

Table 2. Eigenvalues for $V(r) = r$.

N	n	$l=0$	$l=1$	$l=2$
10	0	2.338 107 415/0	3.361 254 8/5	4.248 182 30/26
	1	4.087 953/49	4.884 458/2	5.629 716/08
	2	5.520 7/6	6.207 7/6	6.869 0/89
	3	6.793/87	7.415/06	8.021/10
50	0	2.338 107 410 46	3.361 254 522 98	4.248 182 257 16
	1	4.087 949 444 13	4.884 451 844 10	5.629 708 376 96
	2	5.520 559 828 10	6.207 623 293 69	6.868 882 268 94
	5	9.022 650 853 34	9.557 615 912 82	10.086 459 801 79
	10	13.691 489 035 21	14.123 110 887 62	14.553 890 963 61
	15	17.661 300 106 2/57	18.040 021 868/7	18.418 952 958/6
	20	21.224 89/3	21.569 58/5	21.914 82/77
	25	24.57/1	24.88/3	25.19/5

Results with the Laguerre mesh/exact results from calculations with $N = 70$ and 80.

sum rule

$$\sum_{i=1}^{N} x_i = N(N+\alpha). \tag{4.3}$$

For $N = 10$, the first eigenvalue is obtained to about 10^{-7} ($h = 0.15$), the second one to about 10^{-4} and the third one to about 10^{-3}. These accuracies are found independently of the α value. For $N = 50$, the $n = 0$–11 eigenvalues present the accuracy on the Laguerre zeros. Beyond $n = 11$, the order of magnitude of the absolute error on the nth eigenvalue is roughly given by

$$\varepsilon_n \approx 10^{n-22}.$$

Again, this result is almost independent of m (two dimensions) or l (three dimensions).

In order to appreciate the quality of the results obtained with the Laguerre meshes, we have performed calculations with a cartesian mesh for the three-dimensional harmonic oscillator with $l = 0$. With $N = 50$, neither the 3-point nor the 9-point differentiation formulae were able to provide meaningful results. The lack of validity of the cartesian mesh is explained by the fact that the boundary condition at $r = 0$ is not satisfied. Then we have performed a constrained calculation in which the wavefunction vanishes at the origin. With $N = 50$, a few eigenvalues were obtained with an accuracy poorer than 10^{-2}. These rather negative results show that the cartesian mesh should not be utilised for the polar and radial coordinates. The importance of correcting for the boundary condition has been emphasised by Hoodbhoy and Negele (1977). But even with a correction, the cartesian mesh does not provide very accurate results.

4.4. Linear central potential

For the linear central potential $V(r) = r$, the Laguerre mesh provides fully *variational* results. Indeed, for this potential, formula (2.13) is not an approximation. The N-point mesh calculation with $\alpha = 2l+2$ is thus exactly equivalent to a variational calculation with $r^{l+1}\exp(-\frac{1}{2}r)L_k^{2l+2}(r)$ ($k = 0$ to $N-1$) as basis functions. Contrary to the harmonic oscillator case, these basis functions are not eigenfunctions of the Hamiltonian.

For $l = 0$, the eigenvalues corresponding to the linear potential are the zeros of the Airy function. With ten discretisation points ($h = 0.2$), the accuracy on the first eigenvalue is better than 10^{-8} with the Laguerre mesh (see table 2). Four eigenvalues are significant. With $N = 50$ ($h = 0.2$), sixteen eigenvalues are obtained with an accuracy better than 10^{-10}. The same level of accuracy is obtained for the other l values. Our results agree to better than 10^{-11} with the accurate values of table 8 in Fernandez *et al* (1985).

The results obtained with the modified Laguerre mesh are not as good but remain fair. (The Gauss formula is no more exact in the present case.) With $N = 50$, ten eigenvalues are obtained with a 10^{-5} accuracy for $h = 1.0$.

4.5. Hydrogen atom

We have studied the potential $V(r) = -2/r$ with the Laguerre basis. The relative error on the eigenvalues is presented in figure 2. The results for $l = 0$ are relatively disappointing. If the scale parameter is optimised on the ground state energy, the error is smaller than 5×10^{-3} ($N = 10$, $h = 0.20$) or 2×10^{-5} ($N = 50$, $h = 0.06$). Notice that the function φ_0 is an exact eigenfunction of the Hamiltonian for $h = 2$. However, the error introduced by the Gauss approximation (3.11) is much larger here than in the harmonic oscillator case. It is also possible to adjust the scale parameter to obtain a better relative accuracy for the excited states than for the ground state. In this case, the scale parameter simulates the slower $\exp(-r/n+1)$ decrease of excited states. A compromise is presented in figure 2: with 50 discretisation points, six eigenvalues are obtained with a relative error smaller than 10^{-2} for $h = 1.2$.

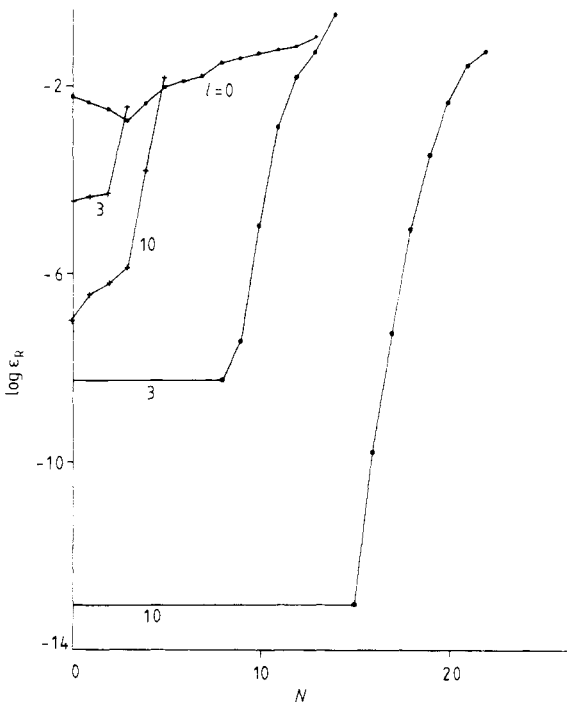

Figure 2. Relative error on the eigenvalues of the Coulomb potential obtained with a mesh based on the Laguerre polynomials. The crosses and the dots respectively correspond to a 10 and a 50 mesh point calculation.

The situation is more favourable for higher l values since the exponentials in the exact hydrogen atom eigenstates differ less strongly. The $l=3$ and $l=10$ examples are displayed in figure 2. For $N=10$ ($h=2.0$) and for $N=50$ ($h=2.4$), respectively, four and twelve accurate $l=3$ eigenvalues are obtained. In both cases, the energy of the $n=0$ eigenvalue can be improved by reducing h, at the cost of a smaller number of significant eigenvalues. Still better results are obtained for $l=10$. With ten discretisation points, more than half the eigenvalues are meaningful ($h=7.5$). With $N=50$, sixteen eigenvalues are obtained to the accuracy of Laguerre zeros ($h=8$).

Finally, notice that by using odd α values, one can easily study the two-dimensional hydrogen atom.

5. Applications to nuclear Hartree–Fock problems

We present here two applications of the method introduced in this paper to problems which have already been studied on a 3D cartesian mesh using conventional finite-difference formulae. Both applications concern nuclear systems. Codes have indeed already been developed to calculate the binding energies of triaxial nuclei (Bonche *et al* 1985) and to restore the rotational invariance of nuclear wavefunctions (Baye and Heenen 1984). The differentiation formulae introduced in § 3.1 can therefore be easily tested in these cases.

5.1. Calculation of the Hartree–Fock energies of spherical nuclei

The Hartree–Fock energies of magic nuclei can be determined very accurately by a 1D spherical code. The energies obtained for these spherical configurations constitute a very good test of the 3D cartesian codes. We have calculated the Hartree–Fock wavefunctions of four nuclei with a code using a 9-point formula for the second derivative. The differentiation formula (3.5) has then been used to calculate more accurately the binding energies corresponding to these wavefunctions. Such a calculation is quasi-variational, but is not fully self-consistent. The values obtained for ^{16}O, ^{40}Ca, ^{90}Zr and ^{208}Pb are given in table 3. The nuclear interaction S 3 has been used and the mesh size is taken equal to 1 fm. (For details of the calculation, see Bonche *et al* (1985).) The binding energies obtained with a 9-point formula overestimate the exact energy by roughly 0.5%. Using formula (3.5), the binding energies obtained in the four cases are lower than the exact one (as it has to be for a variational calculation) with an error of 0.1%. This gain in accuracy is obtained with a very small increase in the computational time, since the calculation of the total energy requires only a small amount of the time necessary to perform a full self-consistent calculation. We think

Table 3. Hartree–Fock energies (in MeV) of spherical nuclei. The energies are calculated with the interaction S3 and: 1, a spherical Hartree–Fock code; 2, a 3D cartesian code using formula (3.5) for the kinetic energy; 3, a 3D cartesian code using a 9-point finite difference formula for the kinetic energy.

	^{16}O	^{40}Ca	^{90}Zr	^{208}Pb
1	128.27	341.92	782.73	1636.61
2	128.26	341.51	781.84	1634.89
3	128.74	343.32	786.14	1645.19

that these energies would still be significantly improved if the formula (3.5) was used in the iteration procedure which determines the self-consistent wavefunction. This however would increase the computing time in a non-negligible way.

5.2. Restoration of rotational invariance

In most cases, a Slater determinant is not rotationally invariant. This invariance can be restored by projection techniques on angular momentum. A method to project wavefunctions discretised on a mesh has been recently set up and applied to rotating nuclei (Baye and Heenen 1984). This method is based on the approximation of rotation operators by matrices acting on the mesh. Let us summarise its main features.

The exact angular momentum operator $\hat{L}_z$

$$\hat{L}_z = -\mathrm{i}(x\,\partial/\partial y - y\,\partial/\partial x) \tag{5.1}$$

can be approximated on the mesh by a matrix $\tilde{L}_z$ constructed by replacing the coordinates x and y, and the first-order derivatives by their representation on the mesh (a tilde indicates the representation on the mesh of an exact operator). The eigenvalues and eigenvectors of $\tilde{L}_z$ can then be used to build a matrix approximation of the rotation operator around the z axis:

$$\tilde{R}(\alpha) = \exp(\mathrm{i}\alpha\tilde{L}_z). \tag{5.2}$$

A 3D rotation is then obtained as a succession of three 2D rotations.

The matrices $\tilde{L}_z$ and $\tilde{R}(\alpha)$ have a dimension $N_x \times N_y$, where N_x and N_y are the number of points along the x and y axes. For a realistic calculation, this dimension becomes very large. However, symmetry considerations enable one to divide $\tilde{L}_z$ in four disconnected blocks, corresponding to even and odd parities and to positive and negative eigenvalues. The eigenvalues of positive (negative) parity approach the even (odd) eigenvalues of the operator $\hat{L}_z$.

As in Baye and Heenen (1984) (to be referred to as BH), we have studied the properties of $\tilde{L}_z$ for a cartesian mesh, but using this time the optimal differentiation formula deduced from (2.10) and (3.4) for this mesh:

$$\Psi'(i) = \frac{\pi}{N} \sum_{j \neq i} \Psi(j) \frac{(-1)^{i-j}}{\sin[\pi(i-j)/N]} \tag{5.3}$$

where i is defined as in § 3.1.

The positive eigenvalues obtained for a mesh with 16 points in each direction are given for both parities in table 4. They correspond to the diagonalisation of a matrix of dimension 64. Half the eigenvalues are good approximations of the exact ones. This number of accurate eigenvalues is nearly twice as large as in BH (see table II of BH). A similar level of improvement can be seen by comparing the eigenvectors drawn in figures 3 and 4 with figure 2 of BH. The real parts of eigenvectors are depicted in a 8×8 box. They represent approximations of the real part of eigenfunctions of $\hat{L}_z$ restricted to the first quadrant. The evolution of the angular nodal lines when the eigenvalue increases can be clearly seen in figure 3, where the best approximations of odd eigenvalues for $m = 1$–19 are drawn. These angular nodal lines correspond to the zeros of $\cos m\varphi$. The eigenvectors approaching the $m = 2$ eigenvectors are represented in figure 4. They have in common a $\varphi = 45°$ nodal line, and they differ by their radial parts, the number of radial nodal lines varying from 0–5.

A very good check of the accuracy of mesh rotations can be performed by rotating a wavefunction with a definite parity by a multiple of π. The approximate rotation

Table 4. Eigenvalues of the matrix $\tilde{L}_z$.

Positive parity							
0	0	0	0	0	0	0	0
1.6617	1.9682	1.9985	2.0000	2.0000	2.0000	2.0000	3.5265
3.7292	3.9732	3.9988	4.0000	4.0000	4.0000	5.0210	5.9201
5.9880	5.9997	6.0000	6.0000	6.3687	6.8850	7.9951	7.9978
8.0000	8.0000	8.4796	9.0236	9.4956	9.9998	10.0000	10.0000
10.1806	12.0000	12.0005	12.0280	12.0339	12.1179	13.2118	14.0001
14.0089	14.0131	15.8905	16.0007	16.0089	16.0430	17.9023	18.0106
18.1379	19.9477	20.6880	20.9373	22.0672	22.8147	26.5271	26.7131
Negative parity							
1.0000	1.0000	1.0000	1.0000	1.0002	1.0045	1.0672	1.4425
2.1876	3.0000	3.0000	3.0000	3.0003	3.0088	3.0662	3.1227
3.9239	4.3173	5.0000	5.0000	5.0001	5.0041	5.0746	5.6778
6.0812	6.2959	7.0000	7.0000	7.0009	7.0209	7.2016	8.3857
8.9995	9.0000	9.0001	9.0352	9.0512	9.7666	10.8838	11.0000
11.0001	11.0063	11.6423	12.2817	13.0000	13.0018	13.1098	14.4144
15.0003	15.0222	15.7633	16.1023	16.1139	17.0035	17.1961	18.4892
19.0138	20.8540	20.9091	21.0120	23.0056	25.1352	27.6393	30.4732

The underlined eigenvalues are accurate approximations of the eigenvalues of the exact operator $\hat{L}_z$.

operator is not unitary and does not conserve the norm and the energy in such a rotation. Table 5 shows that our new formula improves the accuracy by more than an order of magnitude for a Hartree-Fock wavefunction of a rotating ^{24}Mg (for the details of the calculation, see BH).

Let us also note that the projected energies obtained in BH for ^{24}Mg are modified by about 200 keV with respect to about 200 MeV by our improved rotation formula. This modification of 0.1% corresponds to the estimate in BH of the mesh projection error. The error of our new rotation technique can be estimated from table 5 to be less than 0.01%. It indicates that the projection on angular momentum can be performed very accurately on a mesh. Let us finally stress that the introduction of formula (5.3) does not complicate at all the diagonalisation of the operator $\tilde{L}_z$ and the construction of $\tilde{R}(\alpha)$.

6. Conclusion

In this paper, we have presented a new approach to mesh calculations. Equations on particular meshes are derived as an accurate approximation of a variational calculation. This new approach provides an explanation for the unexpected accuracy of a number of Hartree-Fock calculations performed on the cartesian mesh. But besides this explanation, it has several interesting aspects.

(i) The variational nature of the calculation provides accurate upper bounds of the exact energies. Examples show that a large number of significant eigenvalues can be obtained.

(ii) Different types of meshes are proposed. The mesh can be adapted to the coordinate system optimally suited to the problem. The quality of the results depends only on the adequacy of the variational basis from which the mesh is derived.

(iii) For every type of mesh, a coherently defined formula for the kinetic energy is derived. We have shown that with this consistent formula, the error on cartesian

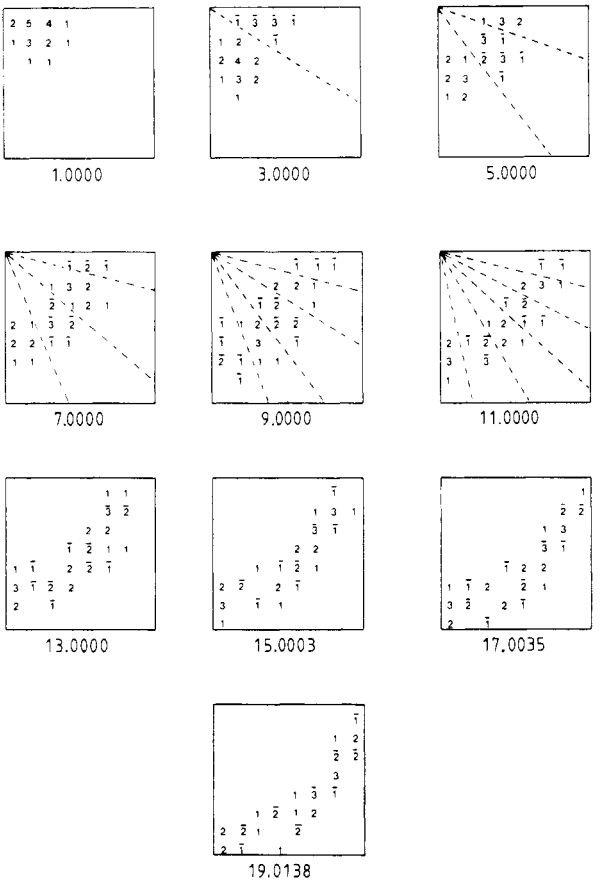

Figure 3. Real part of the eigenvectors corresponding to the odd eigenvalues of $\tilde{L}_z$ without radial nodal lines. The 64 components are multiplied by 10 and truncated of their decimal part. The negative eigenvalues are written with an overbar. The angular nodal lines are shown with broken lines.

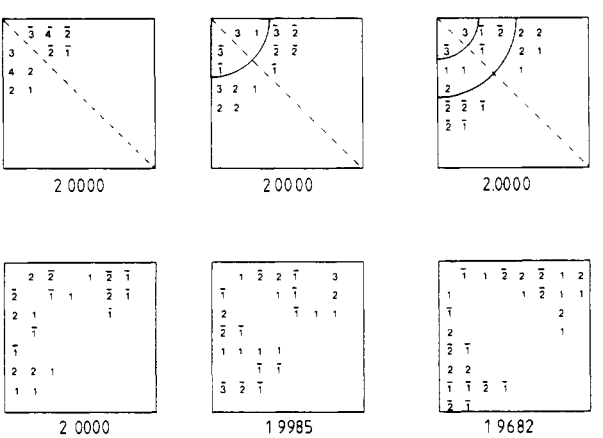

Figure 4. As figure 3 for the eigenvectors corresponding to eigenvalues approaching $2\hbar$.

Table 5. Evolution of the norm and the energy of a ^{24}Mg wavefunction for $n\pi$ rotations.

	$\langle\Psi\|\tilde{R}(\alpha)\|\Psi\rangle$				$-\langle\Psi\|\tilde{H}\tilde{R}(\alpha)\|\Psi\rangle$			
α	Modulus		Phase		Modulus		Phase	
	1	2	1	2	1	2	1	2
0	1.000	1.000	0.000	0.000	185.72	185.72	0	0
π	0.983	0.999	−0.037	0.000	182.47	185.56	−0.036	0.000
2π	0.971	0.998	−0.070	0.000	180.32	185.39	−0.069	0.000
3π	0.956	0.998	−0.100	0.001	177.65	185.26	−0.099	0.001
4π	0.942	0.997	−0.128	0.001	174.87	185.21	−0.125	0.000
5π	0.933	0.997	−0.156	0.000	173.36	185.12	−0.154	0.000
6π	0.915	0.996	−0.182	0.000	170.04	185.05	−0.179	0.000
7π	0.897	0.996	−0.205	0.000	166.85	185.03	−0.202	0.000
8π	0.882	0.996	−0.225	0.001	164.01	184.98	−0.222	0.000

Column 1 corresponds to a 9-point approximation of the first derivative and column 2 to formula (5.3).

mesh calculations is reduced by several orders of magnitude, compared to usual discretisation methods based on Taylor expansion.

(iv) Analytical approximations are obtained for the wavefunctions. They can be employed to compute diagonal and non-diagonal matrix elements accurately. Traditional mesh calculations only provide the values of the wavefunction at the mesh points.

These improvements have been obtained without loss of the simplicity, which is the main advantage of mesh calculations. No matrix elements need to be calculated. The kinetic energy matrix element is determined analytically once for each mesh. Several problems remain open. Are there other types of mesh than those associated with polynomials orthogonal on an interval or polynomials orthogonal on the unit circle? Should other meshes be sought for the cartesian, cylindrical and spherical coordinate systems? A theoretical estimate of the error on the eigenvalues would also be necessary.

The present mesh techniques are expected to be useful in many applications. Accurate ground state and excited state energies should be obtainable for three-dimensional Schrödinger equations by combining different meshes well adapted to the selected coordinate system. The results of Hartree-Fock and time-dependent Hartree-Fock calculations must also be improved if the kinetic energy formula consistent with the cartesian mesh is employed. More spectacular improvements must even be expected for calculations in cylindrical coordinates for which we propose more appropriate meshes than the cartesian mesh.

Acknowledgment

We would like to thank the FNRS for a grant for computation to perform the Hartree-Fock calculations.

References

Abramowitz M and Stegun I A 1965 *Handbook of Mathematical Functions* (New York: Dover)
Bakhvalov N 1973 *Méthodes Numériques* (Moscow: Mir)

Baye D and Heenen P-H 1984 *Phys. Rev.* C **29** 1056-68
Bonche P, Flocard H, Heenen P-H, Krieger S J and Weiss M S 1985 *Nucl. Phys.* A **443** 39-63
Fernandez F M, Meson A M and Castro E A 1985 *J. Phys. A: Math. Gen.* **18** 1389-98
Flocard H, Koonin S E and Weiss M S 1978 *Phys. Rev.* C **17** 1682-99
Hoodbhoy P and Negele J W 1977 *Nucl. Phys.* A **288** 23-44
Marcos S, Flocard H and Heenen P-H 1983 *Nucl. Phys.* A **410** 125-36
Negele J W 1982 *Rev. Mod. Phys.* **54** 913-1015
Sandhya Devi K R and Garcia J D 1983 *J. Phys. B: At. Mol. Phys.* **16** 2837-47
Szegö G 1967 *Orthogonal Polynomials* (Providence, RI: Am. Math. Soc.)